Microwave Assisted Sintering and Photoluminescence Properties of $Ba_3Si_6O_{12}N_2:Eu^{2+}$ Green Phosphors

HAN Bin[1,2], WANG Yi-Fei[1], LIU Qian[3], HUANG Qing[1]

(1. Structural and Functional Integration of Ceramics Group, the Division of Functional Materials and Nanodevices, Ningbo Institute of Materials Technology and Engineering, Chinese Academy of Sciences, Ningbo 315201, China; 2. Institute of Materials, Shanghai University, Shanghai 200072, China; 3. State Key Laboratory of High Performance Ceramics and Superfine Microstructure, Shanghai Institute of Ceramics, Chinese Academy of Sciences, Shanghai 200050, China)

Abstract: Eu^{2+}-doped $Ba_3Si_6O_{12}N_2$ green phosphors were prepared by microwave assisted sintering method at 1275℃ for 4 h, while the counterparts using conventional solid-state reaction method were synthesized at temperature higher than 1300℃ and for to 10 h. Microwave assisted sintering could reduce the activation energy and enhance the diffusion rate, thus greatly improved the sintering. Moreover, the influence of Si_3N_4 content on phase formation, morphology, absorption, and quantum efficiency, and photoluminescence properties of phosphors were studied. As a result, the $Ba_3Si_6O_{12}N_2:Eu^{2+}$ samples sintered by microwave assisted sintering method have a higher phase purity and photoluminescence intensity under ultraviolet excitation as compared with samples sintered in the conventional tube furnace. The proposed method is a potential preparation method for the oxynitride phosphors with strong photoluminescence and high phase purity.

Key words: $Ba_3Si_6O_{12}N_2:Eu^{2+}$ phosphors; oxynitride; microwave assisted sintering; photoluminescence

The phosphor-converted light-emitting diodes (pc-LEDs), emerging as an indispensable solid-state light source for illumination, have attracted increasing attention due to its high efficiency, energy savings, environment-friendliness, small volume and long lifetime, compared with the conventional incandescent and fluorescent lamps[1-2]. Phosphors as a wavelength converter have been considered as pivotal and technologically important components in white LEDs[2]. A new hot topic of nitride and oxynitride phosphors has recently attracted much attention[3–9]. Many rare-earth activated nitride and oxynitride phosphors such as Ca-α-SiAlON: Ce^{3+}[6], β-SiAlON: Eu^{2+}[7], CaAlSiN$_3$:Eu^{2+}[9], $Ba_3Si_6O_{12}N_2:Eu^{2+}$[10–13] have been designed and studied. Among the oxynitride phosphors, the M-Si-O-N (M=Ca, Sr, Ba) system has attraction as a new phosphor system due to its easy fabrication, good thermal stability, and high luminescence efficiency. However, the $MSi_2O_2N_2:Eu^{2+}$ phosphor in the system is not an efficient phosphor with high color purity. It has to be emphasized that $Ba_3Si_6O_{12}N_2:Eu^{2+}$ phosphor has a similar crystal structure and chemical formula to a N-rich $Ba_3Si_6O_9N_4:Eu^{2+}$, but the optical properties are quite different between them. In addition, the $Ba_3Si_6O_{12}N_2$: Eu^{2+} phosphor also shows a high efficiency and a good thermal stability compared with other green phosphors such as (Ba, Sr)$_2$SiO$_4$:Eu^{2+}[13].

Up to now, several methods have been used to synthesize the high efficiency $Ba_3Si_6O_{12}N_2:Eu^{2+}$ phosphors, for instance, gas reduction nitridation method[11], solid state reaction method[12], and $Ba_3SiO_5:Eu^{2+}$ precursor method[13]. However, a pure phase of $Ba_3Si_6O_{12}N_2$ is hardly obtained, due to the low chemical reactivity of starting powders Si_3N_4[6]. And more, these fabrication methods mentioned above are not energy-saving, with disadvantages of long heating time as well as long duration time which can influence the particles morphology and optical features of the product. To overcome the sintering difficulty for $Ba_3Si_6O_{12}N_2:Eu^{2+}$ systems, this study employed microwave sintering (MWS) method by increasing the chemical reactivity and enhancing the diffusion of ions. The microwave sintering method is developed as a new tool in powder manufacture industries.

Received date: 2014-09-28; **Modified date:** 2014-12-08; **Published online:** 2015-01-10

Foundation item: Zhejiang Provincial Natural Science Foundation, China (R12E020005, LQ14E020007); Ningbo Natural Science Foundation, China (2013A610027); Opening Project of State Key Laboratory of High Performance Ceramics and Superfine Microstructure (SKL201307SIC); Research Fund for the Postdoctoral Advanced Program of Zhejiang Province (BSH1301022)

Biography: HAN Bin(1991–), male, candidate of master degree. E-mail: hanbin@nimte.ac.cn

Corresponding author: WANG Yi-Fei, assistant professor. E-mail: wangyf@nimte.ac.cn; HUANG Qing, professor. E-mail: huangqing@nimte.ac.cn

During the heating process, the electromagnetic wave can penetrate into materials and heat them owing to the interaction between polarized molecular (or ions) and electromagnetic field, finally resulting in volumetric heating. The volumetric heating ability of microwaves allows for a more rapid and uniform heating, then decreases processing time, and finally enhances material properties[14-16]. For the Si_3N_4 systems, microwave heating has been observed to accelerate or enhance diffusion processes, such as sintering and grain growth[17]. In this study, $Ba_3Si_6O_{12}N_2$:Eu^{2+} green phosphors were synthesized by the microwave sintering method, as well as solid state reaction (SSR) method for comparison, and their photoluminescence (PL) properties, absorption and quantum efficiency of the phosphors were investigated. The influence of the contents of Si_3N_4 in raw materials and duration time of microwave sintering on the PL properties and phase purity were also discussed.

1 Experiment

1.1 Preparations

Green phosphors ($Ba_{2.8}Si_6O_{12}N_2$: $0.2Eu^{2+}$) were synthesized at 1275℃ for 4 h using starting powders of $BaCO_3$ (Aladdin, AR), SiO_2(Aladdin, 99.99%), Si_3N_4(UBE, SN-E10), and Eu_2O_3(Sinopharm Chemical Reagent Co., Ltd, 4N). The weighted raw powders were mixed in a mortar by hand and packed into the BN crucibles. For the microwave sintering technique, firstly, we put the filled BN crucible into an attemperator with heating assistant materials, then put the attemperator into microwave reaction furnace, and finally sintered the powder samples under a reducing atmosphere (15%H_2/N_2). For comparison, the same samples were prepared by the solid state reaction method, in which the samples were loaded into a conventional alumina tubular furnace and sintered at 1300℃ for 10 h at the same reducing atmosphere in a flowing gas mixture (15%H_2/N_2). Furthermore, to investigate the influence of Si_3N_4 content on the final phase formation in MWS process, the Si_3N_4 content of raw materials was varied with a wide range from 0.6 to 1.0. In order to keep the amount of Si constant in the formular of $Ba_{2.8}Si_6O_{12}N_2$: $0.2Eu^{2+}$, the SiO_2 content was decreased accordingly. In addition, the effect of soaking time (2, 4, and 6 h respectively) on final phase formation was evaluated for the MWS. Post-treatments of the phosphor were also conducted with the aim to improve the PL properties. The treatments include powder smashing and acid washing.

1.2 Characterization

The crystalline phase of the samples was analyzed by an X-ray powder diffraction (XRD, Advance D8, Bruker, Karlsruhe, German) using the Cu Kα, λ= 0.15418 nm, operating at 40 kV and 40 mA in the 2θ range of 10°–60° with a step size of 0.02° and 0.2 s per step. The PL spectra were measured at room temperature using a fluorescent spectrophotometer (F-4600, Hitachi Ltd., Tokyo, Japan) with a 150W Xe lamp as an excitation source at room temperature. The absorption and quantum efficiency of the prepared phosphor were measured using a QE-2100 (Otsuka Electronics Co., Ltd., Japan) and the reflection spectrum of $BaSO_4$ white standards was used for calibration. The particle size was analyzed on a particle size analyzer (S3500-special, Microtrac, USA). The morphology of the samples was observed by scanning electron microscopy (FE-SEM, S-4800, Hitachi, Japan).

2 Results and discussion

2.1 Properties of $Ba_{2.8}Si_6O_{12}N_2$:Eu^{2+} synthesized by MWS and SSR

Figure 1 presents the XRD patterns of $Ba_{2.8}Si_6O_{12}N_2$: $0.2Eu^{2+}$ synthesized by MWS(1275℃, 4 h) and SSR(1300 ℃, 10 h)methods at the stoichiometric ratios of $4.5SiO_2$: $0.5Si_3N_4$ in the starting materials, respectively. As seen from Fig. 1, for the sample prepared by the microwave sintering method, most of the high intensity peaks match well with the reported data by Mikami, *et al*[18], and a few unreacted α-Si_3N_4, orthosilicate phases $BaSi_2O_5$ and $Ba_5Si_8O_{21}$ are still remained. While for the sample prepared by the conventional solid-state reaction method, many weak diffraction peaks of impurities are detected, which also can be identified as α-Si_3N_4, orthosilicate phases $BaSi_2O_5$, $Ba_4Si_6O_{10}$ and $Ba_5Si_8O_{21}$. In addition, the phosphor prepared by the MWS method has higher peak intensity in XRD patterns, indicating that high crystallinity is obtained. Through these results, it is clear that MWS method is a very effective synthesis method as it can reduce processing time to some extent. This may be due to the fact that

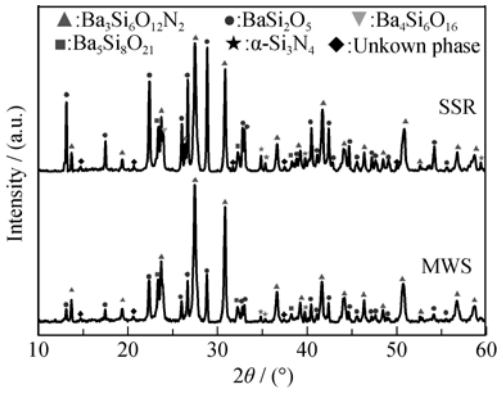

Fig. 1 XRD patterns of $Ba_{2.8}Si_6O_{12}N_2$: $0.2Eu^{2+}$ phosphors synthesized by SSR and MWS methods

strong microwave electric fields induce a nonlinear driving force (named as ponderomotive force) for (ionic) mass transport near surfaces and structural interfaces (*e.g.*, grain boundaries) in ceramic materials[19–21].

The PL excitation spectra of $Ba_{2.8}Si_6O_{12}N_2$: $0.2Eu^{2+}$ phosphors synthesized by SSR and MWS show a typical broad absorption band from near-UV to blue region (300–500 nm), consisting of two bands with maxima at 313 and 428 nm, respectively. While the emission spectra exhibit a single broad band centered at 527 nm under the excitation of λ_{ex}=428 nm, which is attributed to the typical $4f^65d \rightarrow 4f^7$ transition of Eu^{2+} ions. It has been noticed that the emission intensity of the phosphor prepared by the microwave sintering method is higher than that of the phosphor synthesized by the solid state reaction method, as illustrated in Fig. 2. This may be attributed to that the phosphor prepared by the microwave sintering method is endowed with a much pure phase formation of $Ba_3Si_6O_{12}N_2$ having high crystallinity as mentioned above.

The morphologies of the samples prepared by MWS and SSR methods are presented in Fig. 3(a) and 3(b) The particle size is about 3–8 μm for samples prepared by the MWS method, but larger particle size distribution is for SSR method. It can be observed that the particles in the sample prepared by MWS have a fine morphology and regular shape, whereas the appearance of the one prepared by SSR exhibits hard aggregation. The particle size of the phosphors synthesized by the MWS method is effectively modified with the particle size of ~3.04 μm (D_{50}), whereas the SSR phosphor reaches the particle size of ~5.05 μm (D_{50}), as shown in Fig. 3(c) and 3(d). These may be another reason for higher emission intensity of the sample synthesized by MWS, which was addressed in the photoluminescence and morphology of $Ca_3La_3(BO_3)_5$: Eu^{3+} phosphors[22].

Figure 4 shows the absorption, internal and external quantum efficiency of the samples prepared by MWS and SSR methods. The external quantum efficiency of the MWS sample is higher than that of the SSR samples under 365, 405, or 450 nm excitation, respectively. The enhanced quantum efficiency may be due to that the crystallinity of the powders is enhanced by the different preparation method and conditions, resulting in the reduction of the defects in the host lattice and on the surface of the particles. As a result, the possibility of the non-radiation transition within and among the particles is reduced.

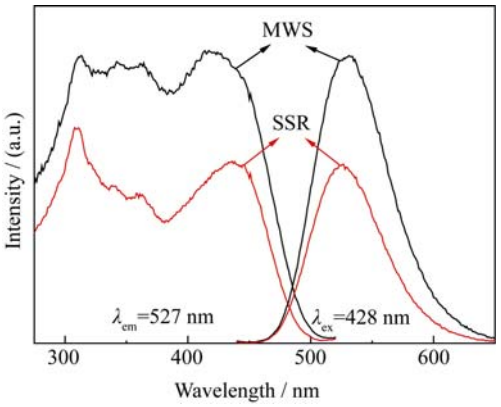

Fig. 2 Excitation and emission spectra of $Ba_{2.8}Si_6O_{12}N_2$: $0.2Eu^{2+}$ phosphor prepared by SSR and MWS methods

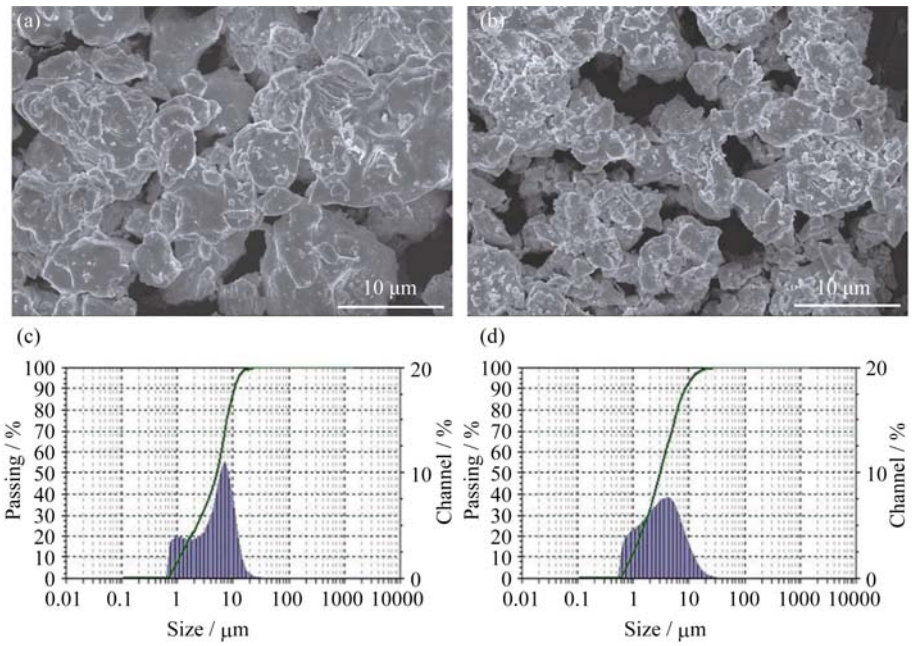

Fig. 3 Micro-morphologies of the samples prepared by (a) SSR and (b) MWS methods, and size distribution of the particles prepared by (c) SSR and (d) MWS methods

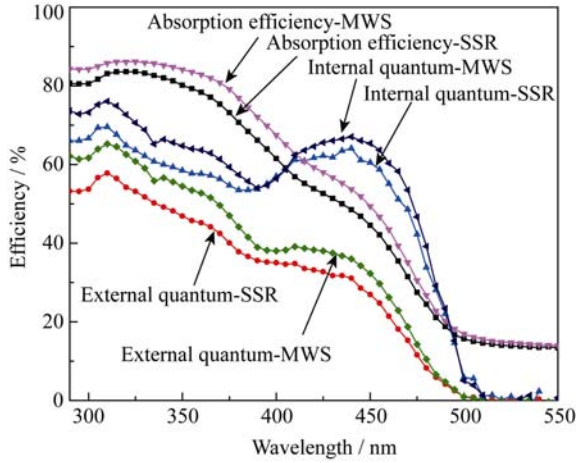

Fig. 4 Absorption, internal and external quantum efficiencies of the samples prepared by MWS and SSR methods

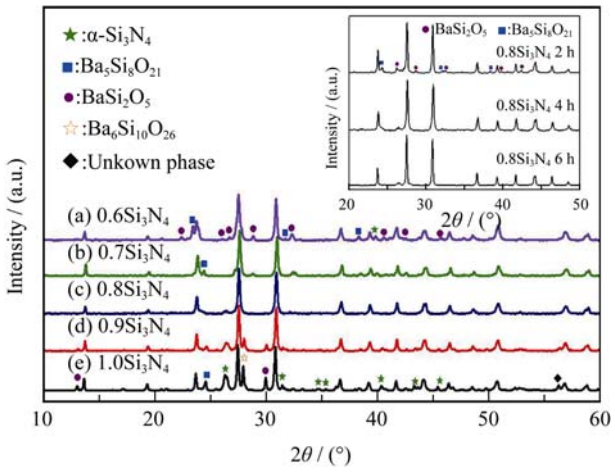

Fig. 5 XRD patterns of $Ba_{2.8}Si_6O_{12}N_2$: $0.2Eu^{2+}$ phosphors as a function of Si_3N_4 content (a) $0.6Si_3N_4$, (b) $0.7Si_3N_4$, (c) $0.8Si_3N_4$, (d) $0.9Si_3N_4$ and (e) $1.0Si_3N_4$, by MWS method at 1275℃ for 4 h. The inset indicates XRD of the sample with $0.8Si_3N_4$ for different soaking time (2, 4, and 6 h, respectively)

2.2 Properties of $Ba_{2.8}Si_6O_{12}N_2:Eu^{2+}$ synthesized by MWS with different ratio of Si_3N_4

Originally for the $Ba_{2.8}Si_6O_{12}N_2$:$0.2Eu^{2+}$ synthesis, the staring host materials were designed as a stoichiometric ratio of $2.8BaCO_3$:$4.5SiO_2$:$0.5Si_3N_4$. However, the stoichiometric mixture of these starting materials yielded much more impurity phase formation of orthosilicate in the final products (as shown in Fig. 1), beyond the expected single $Ba_3Si_6O_{12}N_2$ phase. The resulting oxide formation might be attributed to the deficiency of nitrogen (N), partly because Si_3N_4 commonly contains the oxygen impurity and partly because a gas mixture ($15\%H_2/N_2$) is used in the sintering process[23]. To overcome this problem, the influence of Si_3N_4 content in the starting materials was tested with an increased tendency from 0.6 to 1.0, and in order to keep the amount of Si constant, we decreased the SiO_2 content accordingly. Figure 5 presents the XRD patterns of $Ba_{2.8}Si_6O_{12}N_2$:$0.2Eu^{2+}$ synthesized with difference Si_3N_4 content. All the phosphors were synthesized at 1275℃ for 4 h by the MWS method, indicating that with increasing the content of α-Si_3N_4, orthosilicate phase gradually reduces and transforms into $Ba_3Si_6O_{12}N_2$ when the content of Si_3N_4 is less than 0.8. If the content of Si_3N_4 is above 0.8, the peaks indexed as Si_3N_4 and more diverse orthosilicate phase are detected. According to the reference[10], we can suppose that the phase formation of the $Ba_{2.8}Si_6O_{12}N_2$: $0.2Eu^{2+}$ samples can be composed of three sequential processes: Firstly, the low-melting point barium orthosilicates emerge when the temperature is above 1000℃; Secondly, silicon nitride starts to dissolve in the Ba–Si–O liquid phase when the temperature further rises to 1200–1300℃; Thirdly, the target phase precipitates from the nitrogen saturated liquid phase. As a result, the desired product forms with an excess of silicon nitride and the remained unreacted Si_3N_4 accompanies the formation of barium orthosilicates. The inset in Fig. 5 indicates XRD patterns of the sample with $0.8Si_3N_4$ for different soaking time of 2, 4, and 6 h, respectively. It is clear that a highly pure $Ba_{2.8}Si_6O_{12}N_2$:$0.2Eu^{2+}$ can be realized under MWS conditions at 1275℃ for 4–6 h.

Figure 6 shows the excitation and emission spectra of $Ba_{2.8}Si_6O_{12}N_2$:$0.2Eu^{2+}$ phosphors prepared by MWS method with difference Si_3N_4 contents. As seen in Fig. 6, it shows a great similar shape of the spectra except for the PL intensity, which resulted from the same dominant phase $Ba_3Si_6O_{12}N_2$:$0.2Eu^{2+}$. Because the orthosilicate phases as impurities have no luminescence under blue light irradiation, they only have a negative influence on the PL intensity of the phosphors. The maximum PL intensity is found in the phosphor prepared with a composition of $0.8Si_3N_4$, which owns a highly pure phase and high crystallization degree.

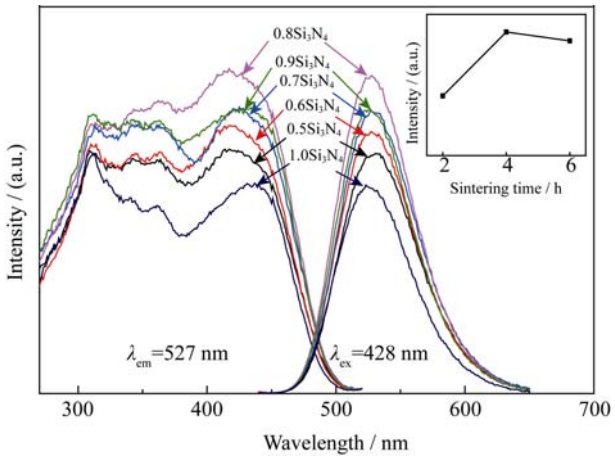

Fig. 6 Excitation and emission spectra of $Ba_{2.8}Si_6O_{12}N_2$: $0.2Eu^{2+}$ phosphors as a function of Si_3N_4 contents, by MWS method at 1275℃ for 4 h. The inset indicating PL intensity of the sample with $0.8Si_3N_4$ for different soaking time (2, 4, and 6 h, respectively)

As shown above, the phase purity plays an important role for enhancing the luminescence intensity of the $Ba_3Si_6O_{12}N_2$:0.2Eu^{2+} phosphors. However, the emission properties are also strongly affected by the particle size and morphology. As seen in Fig. 7, with increasing the Si_3N_4 content, the particle coarsening occurs, thus the particle size increases first and then decreases. Moreover, the particle shape becomes irregular. For instance, the particle size of $Ba_3Si_6O_{12}N_2$:0.2Eu^{2+} phosphor with 0.6Si_3N_4 is ~5 μm with a narrow size distribution. While for the 1.0Si_3N_4 composition, the phosphor exhibits a rough and irregular fracture morphology with an inhomogeneous size distribution. The variation in the particle morphology and particle size distribution can be attributed to the different sintering ability of powders with different compositions. Although Si_3N_4 is stable and not easy to melt during sintering, SiO_2 can act as co-solvent at higher sintering temperatures. So the raw powders with compositions of lower Si_3N_4 content react with other components earlier and more quickly because of the presence of a large amount of the transient liquid phase[24], which would accelerate the material transferring *via* the solution-diffusion-precipitation process. So the influence of Si_3N_4 contents on PL intensity may be attributed to following aspects: i) The stoichiometric ratio of 0.5Si_3N_4 in the starting materials cannot lead to a pure phase formation of $Ba_{2.8}Si_6O_{12}N_2$:0.2Eu^{2+} (Fig. 1) because the SiO_2 layer on the Si_3N_4 surface is not considered or compensated during weighing out of the starting materials; ii) Grain sizedistribution of the phosphor with a high Si_3N_4 content becomes wider (indicated in Fig. 7), then the uneven distribution of the powders leads the scattering enhancement and reduces the luminous efficiency of the phosphor; iii) Diffusion rate of raw materials is lower during the reaction and leads to an incomplete reaction, therefore, the degree of crystallinity is reduced. Besides, the experimental results show that the particles with a uniform shape and a smooth surface had a better PL intensity than that of the particles with an irregular shape and a rough surface[22]. So, combinating the previous formation process of the $Ba_{2.8}Si_6O_{12}N_2$:0.2Eu^{2+}, the phosphor with a 0.8Si_3N_4 starting content is expected to have a higher PL intensity.

Figure 7(c) and (f) presents the morphologies of the phosphor with a 0.8Si_3N_4 starting content before and after post-treatment. We can see that the as-prepared sample (without treatment) shows a large agglomerate consisting of many small particles. While these post-treatments play a role in reducing surface defects, removing the tiny residues, and narrowing the particle size distribution, which has the particle size of ~4.20 μm (D_{50}) in Fig. 8(a), and thus enhance the absorption of the incident light and

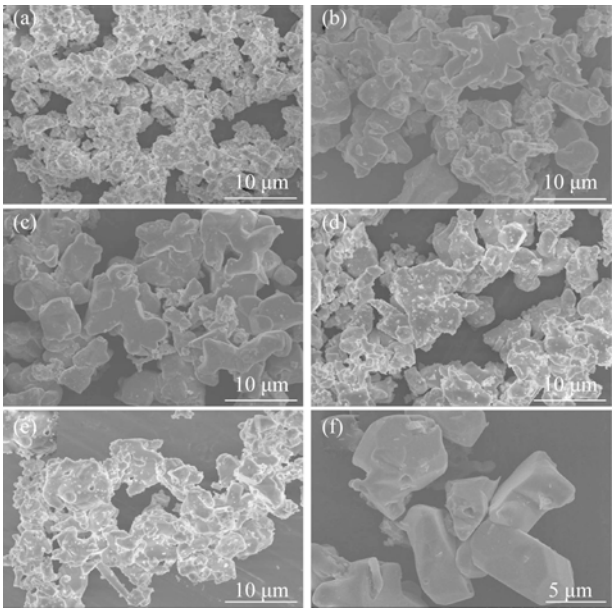

Fig. 7 Morphologies of samples with different Si_3N_4 contents (a) 0.6Si_3N_4, (b) 0.7Si_3N_4, (c) 0.8Si_3N_4, (d) 0.9Si_3N_4, (e) 1.0Si_3N_4 by MWS method at 1275℃ for 4 h, (f) a SEM image of the post-treated sample with 0.8Si_3N_4 by smashing and acid washing

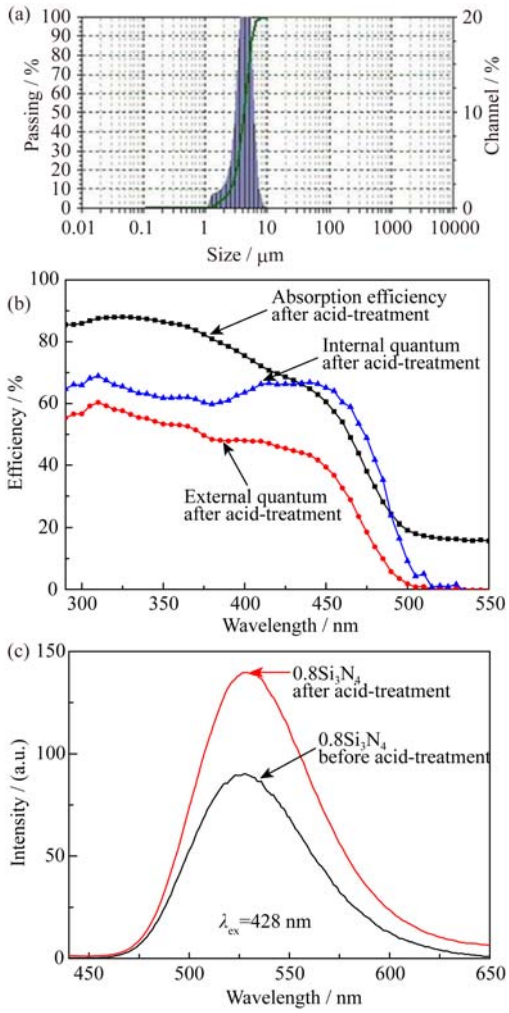

Fig. 8 (a) Particle size distribution of the post-treated sample with 0.8Si_3N_4, (b) absorption and quantum efficiency of the post-treated sample and (c) PL intensity of as-prepared and post-treated sample

decrease the nonradiative transition probability. Figure 8(b) shows the absorption and quantum efficiency of the phosphor after post-treatment. The external quantum efficiency of the samples with $0.8Si_3N_4$ after the acid washing was high, under 365, 405, and 450 nm excitation, respectively. This is most likely due to the reason discussed above. As a results, the particle has a smooth surface (Fig. 7(f)) and the PL intensity is improved after post-treatment (Fig. 8(c)).

3 Conclusions

In summary, Eu^{2+}-doped $Ba_3Si_6O_{12}N_2$ green phosphors were synthesized by both solid state reaction and microwave sintering methods. Comparatively, the microwave sintering method could significantly reduce the firing time for $Ba_3Si_6O_{12}N_2:Eu^{2+}$ phosphors. The highest PL intensity was obtained in the $Ba_{2.8}Si_6O_{12}N_2:0.2Eu^{2+}$ phosphor prepared by microwave sintering method at 1275℃ for 4 h using a $0.8Si_3N_4$ rich composition. Furthermore, the PL intensity could be enhanced greatly by post-treatments of smashing and acid washing. The $Ba_{2.8}Si_6O_{12}N_2:0.2Eu^{2+}$ phosphor with high quantum efficiency and suitable excitation range is a promising stable green phosphor for white LED application. The proposed method is expected to be potentially applicable to other oxynitride phosphors with higher photoluminescence and phase purity.

References:

[1] PUST PHILIPP, WEILER VOLKER, HECHT CORA, *et al*. Narrow-band red-emitting $Sr[LiAl_3N_4]:Eu^{2+}$ as a next-generation LED-phosphor material. *Nature Materials*, 2014, **13:** 891–896.

[2] YE S, XIAO F, PAN Y X, *et al*. Phosphors in phosphor-converted white light-emitting diodes: recent advances in materials, techniques and properties. *Materials Science and Engineering R*, 2010, **71:** 1–34.

[3] LIU JIA-QING, WANG XIAO-JUN, XUAN TONG-TONG, *et al*. Photoluminescence and thermal stability of Mn^{2+} co-doped $SrSi_2O_2N_2:Eu^{2+}$ green phosphor synthesized by Sol-Gel method. *Journal of Alloys and Compounds*, 2014, **593:** 128–131.

[4] XIE RONG-JUN, HIROSAKI NAOTO. Silicon-based oxynitride and nitride phosphors for white LEDs—a review. *Science and Technology of Advanced Materials*, 2007, **8:** 588–600.

[5] LU YA-JUN, WANG HONG-ZHI, LI YAO-GANG, *et al*. Photoluminescence properties of Eu^{2+}, Dy^{3+}, Li^{+} co-doped $CaSi_2O_2N_2$ phosphors. *Journal of Inorganic Materials*, 2012, **27(10):** 1095–1098.

[6] XIE RONG-JUN, HIROSAKI NAOTO, MITOMO MAMORU, *et al*. Photoluminescence of rare-earth-doped Ca-α-SiAlON phosphors: composition and concentration dependence. *Journal of the American Ceramic Society*, 2005, **88(10):** 2883–2888.

[7] HIROSAKI NAOTO, XIE RONG-JUN, KIMOTO KOJI, *et al*. Characterization and properties of green-emitting β-SiAlON:Eu^{2+} powder phosphors for white light-emitting diodes. *Applied Physics Letters*, 2005, **86(21):** 211905.

[8] LI Y Q, HIROSAKI N, XIE R J, *et al*. Photoluminescence properties of rare earth doped α-Si_3N_4. *Journal of Luminescence*, 2010, **130:** 1147–1153.

[9] HU WEI-WEI, CAI CHAO, ZHU QIANG-QIANG, *et al*. Preparation of high performance $CaAlSiN_3:Eu^{2+}$ phosphors with the aid of BaF_2 flux. *Journal of Alloys and Compounds*, 2014, **613:** 226–231.

[10] LI WAN-YUAN, XIE RONG-JUN, ZHOU TIAN-LIANG, *et al*. Synthesis of the phase pure $Ba_3Si_6O_{12}N_2:Eu^{2+}$ green phosphor and its application in high color rendition white LEDs. *Dalton Transactions*, 2014, **43:** 6132–6138.

[11] SONG Y H, KIM B S, JUNG M K, *et al*. Synthesis and photoluminescence properties of green-emitting $Ba_3Si_6O_{12}N_2$ oxynitride phosphor using boron-coated Eu_2O_3 for white LED applications. *Journal of the Electrochemical Society*, 2012, **159(5):** J148–J152.

[12] TANG JIA-YE, CHEN JUN-HUA, HAO LU-YUAN, *et al*.Green Eu^{2+}-doped $Ba_3Si_6O_{12}N_2$ phosphor for white light-emitting diodes: Synthesis, characterization and theoretical simulation. *Journal of Luminescence*, 2011, **131:** 1101–1106.

[13] KANG EUN-HEE, CHOI SUNG-WOO, HONG SEONG-HYEON. Synthesis of $Ba_3Si_6O_{12}N_2:Eu^{2+}$ green phosphors using $Ba_3SiO_5:Eu^{2+}$ precursor and their luminescent properties. *Journal of Solid State Science and Technology*, 2012, **1(1):** R11–R14.

[14] THOSTENSON E T, CHOU TW. Microwave processing: fundamentals and applications. *Composites Part A: Applied Science and Manufacturing*, 1999, **30(9):** 1055–1071.

[15] CLARK DAVID E, FOLZ DIANCE C, WEST JON K. Processing materials with microwave energy. *Materials Science and Engineering*, 2000, **A287:** 153–158.

[16] LIU LI-HONG, ZHOU XIAO-BING, XIE RONG-JUN, *et al*. Facile synthesis of Ca-α-SiAlON:Eu^{2+} phosphor by the microwave sintering method and its photoluminescence properties. *Chinese Science Bulletin*, 2013, **58(7):** 708–712.

[17] TIEGS T N, KIGGANS J O, KIMREY H D. Microwave sintering of silicon nitride. *Ceramic Engineering & Science Proceedings*, 1991, **12(9/10):** 1981–1992.

[18] MASAYOSHI MIKAMI, SATOSHI SHIMOOKA, KYOTA UHEDA, *et al*. New green phosphor $Ba_3Si_6O_{12}N_2$:Eu for white LED: crystal structure and optical properties. *Key Engineering Materials*, 2009, **403:** 11–14.

[19] BOOSKE J H, COOPER R F, FREEMAN S A, *et al*. Microwave ponderomotive forces in solid-state ionic plasmas. *Physics of Plasmas*, 1998, **5(5):** 1664–1670.

[20] BOOSKE JOHN H, COOPER REID F, FREEMAN SAMUEL A. Microwave enhanced reaction kinetics in ceramics. *Materials Research Innovations*, 1997, **1:** 77–84.

[21] WANG YI-FEI, LIU LI-HONG, XIE RONG-JUN, *et al*. Microwave assisted sintering of thermally stable $BaMgAl_{10}O_{17}:Eu^{2+}$ phosphors. *Journal of Solid State Science and Technology*, 2013, **2(9):** R196–R200.

[22] ZHANG YUE, LI YA-DONG, YIN YAN-SHENG. Red photoluminescence and morphology of Eu^{3+} doped $Ca_3La_3(BO_3)_5$ phosphors. *Journal of Alloys and Compounds*, 2005, **400:** 222–226.

[23] PEUCKERT MARCELL, GREIL PETER. Oxygen distribution in silicon nitride powders. *Journal of Materials Science*, 1987, **22:** 3717–3720.

[24] XIE RONG-JUN, MITOMO MAMORU, XU FANG-FANG, *et al*. Preparation of Ca-alpha-sialon ceramics with compositions along the Si_3N_4-1/2Ca_3N_2:3AlN line. *Zeitschrift für Metallkunde*, 2001, **92(8):** 931–936.

微波法合成 $Ba_3Si_6O_{12}N_2:Eu^{2+}$绿色氮氧化物荧光粉及其光学性能研究

韩 斌[1,2], 王义飞[1], 刘 茜[3], 黄 庆[1]

(1. 中国科学院 宁波材料技术与工程研究所, 宁波 315201; 2. 上海大学 材料研究所, 上海 200072; 3. 中国科学院 上海硅酸盐研究所, 高性能陶瓷和超微结构国家重点实验室, 上海 200050)

摘 要: 分别采用微波法和传统固相法制备了 Eu^{2+}掺杂的 $Ba_3Si_6O_{12}N_2$ 绿色氮氧化物荧光粉, 利用 X 射线衍射仪(XRD)、扫描电子显微镜(SEM)、荧光光谱仪等检测方法研究 $Ba_3Si_6O_{12}N_2:Eu^{2+}$的物相、表面形貌及光致发光特性。研究结果表明: 在微波场下 1275℃保温 4 h 合成的 $Ba_3Si_6O_{12}N_2:Eu^{2+}$绿粉的发光强度高于在传统固相法 1300℃保温 10 h 的样品强度。微波辅助烧结可以降低活化能, 从而提高扩散率, 并大大提高了晶体的结晶性。研究了氮化硅含量对物相的形成、形貌和光致发光性能的影响。结果表明: 氮化硅不仅能够促进晶体的结晶度, 而且还能提高其在紫外激发下的发光强度。因此, 微波法有望应用于合成具有高的相纯度和发光强度的其他氮氧化物荧光粉体。

关 键 词: $Ba_3Si_6O_{12}N_2:Eu^{2+}$荧光粉; 氮氧化物; 微波烧结技术; 光致发光

中图分类号: TQ174 **文献标识码:** A